ENTROPY DISSIPATION OF MOVING MESH ADAPTATION

MARIA LUKACOVA-MEDVIDOVA
Johannes Gutenberg University, Mainz, Germany
lukacova@uni-mainz.de

NIKOLAOS SFAKIANAKIS
Johannes Gutenberg University, Mainz, Germany
sfakiana@uni-mainz.de

Tuesday 25th February, 2014

Abstract

Non-uniform grids and mesh adaptation have become an important part of numerical approximations of differential equations over the past decades. It has been experimentally noted that mesh adaptation leads not only to locally improved solution but also to numerical stability of the underlying method.

In this paper we consider nonlinear conservation laws and provide a method to perform the analysis of the moving mesh adaptation method, including both the mesh reconstruction and evolution of the solution. We moreover employ this method to extract sufficient conditions -on the adaptation of the mesh- that stabilize a numerical scheme in the sense of the entropy dissipation.

Keywords: conservation laws, numerical methods, adaptive mesh reconstruction, entropy stability

1 Introduction

Hyperbolic conservation laws appear in various applications. For example, fundamental physical laws, the conservation of mass momentum and energy, lead to the Euler equations of gas dynamics. Further examples arise in traffic flows, shallow water flows, magnetohydrodynamics and biology, see, e.g. [29, 45, 15, 12].

Let us consider a scalar conservation law in one space dimension,

$$u_t + f(u)_x = 0, \quad x \in [a,b],\ t \in [0,T], \tag{1}$$

with initial data $u_0 \in L^\infty([a,b])$. In order to simplify the presentation we assume e.g. periodic boundary conditions or Cauchy problem.

Adaptivity is a main theme in modern computational simulations of complex physical phenomena. It is important to investigate the behavior of adaptive schemes for hyperbolic problems, such as (1), which exhibit several interesting and not trivial characteristics. In literature we can find different mesh adaptation approaches see e.g. [17, 32, 5, 34, 36, 41, 22, 14] and the references therein.

In this work we study the behaviour of certain geometrically driven adaptive algorithms when combined with the important class of entropy conservative schemes introduced in [38, 39].

In every time step $t = t^n$ we consider the following spatial mesh:

$$M_x^n = \{a = x_1^n < \cdots < x_N^n = b\}$$

with variable space step sizes $h_i^n = x_{i+1}^n - x_i^n$, $i = 1, \ldots, N-1$. The mesh will be reconstructed in every time step t^n. Further, we consider a numerical approximation U^n of the exact solution u over the mesh M_x^n at time $t = t^n$ given as a

$$U^n = \{u_1^n, \ldots, u_N^n\}\,.$$

For both the analysis and the numerical studies of this paper we have used a specific kind of mesh adaption techniques that we shortly describe here and in more details in Section 2. Both, the construction and evolution of our non-uniform meshes and the time evolution of the approximate solutions, are dictated by the Main Adaptive Scheme (MAS) :

- in every time step construct new mesh according to the prescribed adaptivity criterion,
- reconstruct the numerical solution over the new mesh,
- evolve the numerical solution in time using the numerical scheme.

MAS will be discussed in details in Section 2; we note here that the number of spatial nodes is fixed and that the reconstruction of the mesh is realized by moving its points according to the geometry of the numerical solution.

The use of non-uniform adaptively redefined meshes, in the context of finite differences, was first studied, among others, in [16], [10], and [40]. The approach that we follow, for the mesh reconstruction step of MAS (Step 1) was first introduced in [4, 1]. Applications of MAS on several problems, point out a strong stabilisation property emanating from the mesh reconstruction see e.g. [6, 3, 5, 36, 35]. These stabilization properties led in [5] to combine MAS with the marginal class of entropy conservative schemes. The later were first introduced by [38] and further studied by [27, 39, 30, 18]. These are semi-discrete numerical schemes which satisfy an exact entropy equality. On one hand entropy conservative schemes are interesting on their own right, since they appear in the context of zero dispersion limits, complete integrable systems and computation of non-classical shocks. On the other hand they are important as building blocks for the construction of entropy stable schemes [38, 39, 30].

We note that classical techniques for the analysis of numerical schemes using moving meshes, only include the time evolution step of the procedure. In order though to have a complete picture of the quality of the numerical solution under a mesh adaptation procedure a broader analysis is needed. In this direction the work done in [35] has provided some constructive analysis tools.

In the present paper we are able to combine in one relation, the effect of both the time evolution and the mesh adaptation used in the moving mesh approach. Let us point out that our approach allows us to represent the effects of both the adaptive mesh reconstruction as well as finite volume scheme in one conservative update relation over a reference uniform mesh (22). This approach allows to apply the entropy stability analysis and derive a sufficient mesh adaptation criterion to control entropy production.

2 Main Adaptive Scheme (MAS)

Using non-adaptive meshes -both uniform and non-uniform- the evolution of the numerical solution is dictated solely by the solution update. On the contrary, in the adaptive mesh case, two more phenomena need to be taken into account; the construction of the new mesh and the solution update. These steps comprise the Main Adaptive Scheme (MAS):

Definition 2.1 (MAS)**.** Given mesh M_x^n and approximations U^n,

1. (Mesh Reconstruction). Construct new mesh M_x^{n+1}
2. (Solution Update). Reconstruct U^n over M_x^{n+1} to obtain $\hat{U}^n$.
3. (Time Evolution). Evolve $\hat{U}^n$ in time to compute U^{n+1} over M_x^{n+1}.

It is important to note that in the case of a fixed mesh, uniform or non-uniform, there is no need for mesh reconstruction (Step 1.) and effectively no need for step 2. In such case MAS reduces to just the time evolution step (Step 3.) which is what is usually considered as a numerical scheme. The extra steps of the adaptive MAS, on one hand, change significantly both the computation and the analysis of the numerical approximations, and on the other hand are responsible for stabilization properties of the MAS.

The crucial property of the mesh adaptation that is analysed in this paper is the following: In the mesh reconstruction step (Step 1.) the nodes of the mesh are relocated according to the geometric information contained in the discrete numerical solution:

in areas where the numerical solution is more smooth and flat the density of the nodes is low, in areas where the numerical solution is less smooth or flat the density of the nodes should be higher.

In fact, the mesh reconstruction process can be chosen in any suitable way. One possibility is to use the monitor function which reflects the curvature of the numerical solution. For details we refer [3, 35].

Further, we consider the solution update procedure (Step 2. of MAS). The numerical solution U^n is given on the old mesh M_x^n and is recomputed as $\hat{U}^n$ on the new mesh M_x^{n+1}. There are many ways for the reconstruction. In this work we use conservative piecewise constant reconstructions.

Finally, for the time evolution step (Step 3. of MAS) we use any suitable numerical scheme for non-uniform meshes. Denoting the mesh-solution pair by

$$U^n = \left\{u_i^n, i = 1, \dots, N\right\} \tag{2}$$

$$M_x^n = \left\{C_i^n, |C_i^n| = h_i^n, i = 1, \dots, N\right\} \tag{3}$$

we obtain in the case of finite volume scheme

$$u_i^{n+1} = \hat{u}_i^n - \frac{\Delta t^n}{h_i^{n+1}}\Big(\hat{F}_{i+1/2}^n - \hat{F}_{i-1/2}^n\Big). \tag{4}$$

Here $\hat{U}^n = \{\hat{u}_i^n, i = 1, \dots, N\}$ is a reconstructed U^n over M_x^{n+1} and the numerical flux F is decorated with $\hat{}$ since it is computed over the updated values $\hat{U}$. The numerical flux itself can be any numerical flux valid for non-uniform grids. We refer to [35, 3] for more details regarding both the implementation of numerical schemes over non-uniform meshes and their properties.

2.1 Reference uniform mesh

A schematic representation of MAS (2.1) in the form of mesh-solution pairs is the following

$$\Big\{M_x^n, U^n\Big\} \xrightarrow{\text{mesh adapt.}} \Big\{M_x^{n+1}, \hat{U}^n\Big\} \xrightarrow{\text{num. scheme}} \Big\{M_x^{n+1}, U^{n+1}\Big\}, \tag{5}$$

where in the first part we have considered the steps 1 and 2 of MAS and in the second part the step 3.

In parallel to MAS and (5) we define a new set of mesh-solution pairs where the meshes are uniform, constant in time, of the same cardinallity as M_x^n and discretizing the same physical domain.

Definition 2.2 (Reference uniform mesh-solution pair)**.** Let $\{M_x, U\}$ and $\{\bar{M}, V\}$ be two mesh-solution pairs with $M_x = \{C_i, |C_i| = h_i,\ i = 1, \dots, N\}$, $\bar{M} = \{\bar{C}_i, |\bar{C}_i| = \Delta x,\ i = 1, \dots, N\}$, $U = \{u_i, i = i, \dots, N\}$, and $V = \{v_i, i = 1, \dots, N\}$. We call $\{\bar{M}, V\}$ the reference uniform mesh-solution pair to $\{M_x, U\}$ if

- the meshes M_x and $\bar{M}$ discretize the same physical domain, and
- the following per-cell mass conservation is satisfied for every $i = 1, \dots, N$

$$\Delta x\, v_i = h_i\, u_i. \tag{6}$$

We prove in Lemma 2.1 that the per-cell conservation property (6) is a result of a geometric conservation law.

Geometric conservation law

Let us consider a a time dependent cell $C(\tau) = (x_1(\tau), x_2(\tau))$. We look for an appropriate conservation law

$$u_t(x,t) + \xi(u(x,t), x)_x = 0, \tag{7}$$

that expresses the mass conservation of a quantity u using an appropriate $\xi(u, x)$ function over the moving cell $C(\tau)$. Thus, by the Leibniz rule

$$\frac{d}{d\tau}\int_{x_1(\tau)}^{x_2(\tau)} u(x,\tau)dx = u(x_2(\tau),\tau)x_2'(\tau) - u(x_1(\tau),\tau)x_1'(\tau) + \int_{x_1(\tau)}^{x_2(\tau)} u_t(x,\tau)dx. \tag{8}$$

If the mass of u over $C(\tau)$ remains constant with respect to τ, the following condition holds

$$\int_{x_1(\tau)}^{x_2(\tau)} u_t(x,\tau)dx = -u(x_2(\tau),\tau)x_2'(\tau) + u(x_1(\tau),\tau)x_1'(\tau). \tag{9}$$

Integrating (7) over $C(\tau)$ we obtain

$$\int_{x_1(\tau)}^{x_2(\tau)} u_t(x,\tau)dx + \int_{x_1(\tau)}^{x_2(\tau)} \xi(u(x,\tau),x)_x dx = 0.$$

Now, using (9) we get

$$\xi(u(x_2(\tau),\tau),x_2(\tau)) - \xi(u(x_1(\tau),\tau),x_1(\tau)) = u(x_2(\tau),\tau)x_2'(\tau) - u(x_1(\tau),\tau)x_1'(\tau).$$

A suitable flux function ξ hence is

$$\xi(u(x(\tau),\tau),x(\tau)) = u(x(\tau),\tau)x'(\tau). \tag{10}$$

Therefore, the strong formulation of (7) reads

$$u_t(x,\tau) + (u(x,\tau)x_t)_x = 0, \tag{11}$$

which is referred in the literature as the Geometric Conservation Law (GCL), see e.g. [46, 44, 7].

As previously announced we can attain the per-cell mass conservation property (6) by discretizing the corresponding GCL.

Lemma 2.1. *The per-cell mass conservation label* (6) *is a consequence of the geometric conservation law* (11).

Proof. For every given cell-value pair C_i, u_i and the respective reference pair $\bar{C}_i$, v_i –as provided in the Definition 2.2– we set the moving cell $C(\tau) = (x_1(\tau), x_2(\tau))$ for $\tau \in [\tau_1, \tau_2]$ to be a linear interpolation of C_i and $\bar{C}_i$

$$C(\tau) = \frac{\tau - \tau_1}{\tau_2 - \tau_1}\bar{C}_i + \frac{\tau_2 - \tau}{\tau_2 - \tau_1}C_i.$$

Now, to attain a discrete version of (11) we integrate it over $C(\tau)$

$$\int_{x_1(\tau)}^{x_2(\tau)} u_t(x,\tau)dx + \int_{x_1(\tau)}^{x_2(\tau)} \left(u(x(\tau),\tau)x_t(x,\tau)\right)_x dx = 0,$$

and invoke (8) to get

$$\frac{d}{d\tau}\int_{x_1(\tau)}^{x_2(\tau)} u(x,\tau)dx - u(x_2(\tau),\tau)x_2'(\tau) + u(x_1(\tau),\tau)x_1'(\tau) + \int_{x_1(\tau)}^{x_2(\tau)} \left(u(x(\tau),\tau)x_t(x,\tau)\right)_x dx = 0.$$

We discretize explicitly in $[\tau_1, \tau_2]$ after noting that $u = u_i$ at $\tau = \tau_1$ and $u = v_i$ at $\tau = \tau_2$, set $\Delta\tau = \tau_2 - \tau_1$, and recall that $|C_i| = h_i$, and $|\bar{C}_i| = \Delta x$ to get

$$\frac{1}{\Delta\tau}(\Delta x v_i - h_i u_i) - u_i\frac{x_2(\tau_2) - x_2(\tau_1)}{\Delta\tau} + u_i\frac{x_1(\tau_2) - x_1(\tau_1)}{\Delta\tau} + u_i\frac{x_2(\tau_2) - x_2(\tau_1)}{\Delta\tau} - u_i\frac{x_1(\tau_2) - x_1(\tau_1)}{\Delta\tau} = 0$$

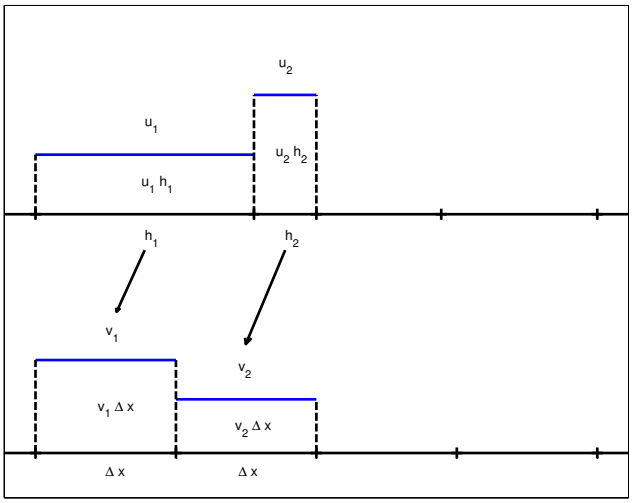

Figure 1: Geometric conservation law projection. The numerical solution over the non-uniform adaptive grid (upper graph) along side with the solution over the reference uniform grid (lower graph). The arrows depict the projection via the corresponding geometric conservation law that results to the per-cell mass conservation. The duration of this projection is described by the fictitious time variable τ.

or simply

$$\Delta x \; v_i = h_i \; u_i.$$

And this concludes the proof of the Lemma. □

Remark 2.1. The time variable τ used in the previous proof refers to ficticious time; it does not correspond to the physically relevant time.

We point out that in the analysis we will use the reference uniform mesh-solution pair to combine the effects of mesh adaptivity and the numerical update.

In view of the Definition 2.2, and after applying the per-cell mass conservation (6) on the schematic representation (5) of MAS, we get for $i = 1, \ldots, N$:

$$h_i^n \; u_i^n = \Delta x \; v_i^n \xrightarrow{\text{mesh adapt.}} h_i^{n+1} \; \hat{u}_i^n = \Delta x \; \hat{v}_i^n \xrightarrow{\text{num. scheme}} h_i^{n+1} \; u_i^{n+1} = \Delta x \; v_i^{n+1}. \tag{12}$$

Now, by invoking (12) after multiplying with h_i^{n+1}, we can rewrite the scheme (4) over the uniform reference mesh

$$v_i^{n+1} = \hat{v}_i^n - \frac{\Delta t^n}{\Delta x} \left(\hat{F}_{i+1/2}^n - \hat{F}_{i-1/2}^n \right), \tag{13}$$

where $\hat{F}$ is the numerical flux function from (4) written in variables $\hat{v}$; and we once again note that this schemes describes only the time update step of the overall scheme.

We refer to Figure 1 for a graphical explanation of the projection between the non-uniform and the uniform reference mesh.

3 Entropy stability

It is a well-known fact that for hyperbolic conservation laws we look for the so called weak entropy solution; i.e. a weak solution that satisfies an entropy inequality. In numerical approximations of (1) a goal is to look for a scheme that automatically produces solutions satisfying a discrete version of entropy inequality. The concept of the so-called entropy stable schemes has been first introduced in [38, 39] and the corresponding numerical solution then satisfies the per-cell entropy inequality. If for every cell just discrete entropy equality is satisfied, such scheme is named entropy stable scheme. We refer to [38, 39, 18, 27] for further details.

Before stating the main theoretical result we introduce the following notations:

$$\Delta v^n_{i+1/2} := v^n_{i+1} - v^n_i, \tag{14a}$$

$$B^n_{i+1/2} := \frac{f(v^n_{i+1}) - f(v^n_i)}{\Delta v^n_{i+1/2}}, \tag{14b}$$

$$Q^n_{i+1/2} := \frac{f(v^n_{i+1}) + f(v^n_i) - 2\hat{F}^n_{i+1/2}}{\Delta v^n_{i+1/2}}, \tag{14c}$$

$$\Delta x^{n+1/2}_{i+1/2} := x^{n+1}_{i+1/2} - x^n_{i+1/2}, \tag{14d}$$

$$H^n_{i+1/2} := \frac{\left(\Delta x^{n+1/2}_{i+1/2}\right)_-}{h^n_i} v^n_i - \frac{\left(\Delta x^{n+1/2}_{i+1/2}\right)_+}{h^n_{i+1}} v^n_{i+1}, \tag{14e}$$

$$M^n_i := \tilde{v}^n_i \left(H^n_{i-1/2} - H^n_{i+1/2}\right). \tag{14f}$$

Now, we proceed with the main theoretical result.

Theorem 3.1. *We use the notations* (14a)-(14f) *and assume that the following condition holds*

$$M^n_i \le \frac{\Delta t^n}{4\Delta x}\Bigg\{\left(D^n_{i-1/2} - K^3\frac{\Delta t^n}{\Delta x}\left(B_{i-1/2} + Q^*_{i-1/2} + D_{i-1/2}\right)^2\right)(\Delta v^n_{i-1/2})^2 + \left(D^n_{i+1/2} - K^3\frac{\Delta t^n}{\Delta x}\left(B_{i+1/2} - Q^*_{i+1/2} - D_{i+1/2}\right)^2\right)(\Delta v^n_{i+1/2})^2\Bigg\}, \tag{15}$$

where Δx, Δt^n *are respectively the space and time steps that correspond to the numerical scheme* (4). Q^* *is the numerical viscosity of an entropy conservative scheme (see also Appendix A and [39] for the definition and some properties of* Q^**). Then the mesh adaptation procedure MAS* (5) *with the numerical scheme* (4) *for the time evolution step is entropy stable.*

Proof. The numerical scheme for the uniform variables reads, cf. (13)

$$v^{n+1}_i = \hat{v}^n_i - \frac{\Delta t^n}{\Delta x}\left(\hat{F}^n_{i+1/2} - \hat{F}^n_{i-1/2}\right).$$

We subtract v^n_i to develop the respective incremental form

$$v^{n+1}_i - v^n_i = \hat{v}^n_i - v^n_i - \frac{\Delta t^n}{2\Delta x}\left(2\hat{F}^n_{i+1/2} - 2\hat{F}^n_{i-1/2}\right).$$

Equivalently

$$
\begin{aligned}
&v_i^{n+1} - v_i^n \\
&\quad = \hat{v}_i^n - v_i^n - \frac{\Delta t^n}{2\Delta x}\Bigg(f(v_{i+1}^n) + f(v_i^n) - \frac{f(v_{i+1}^n) + f(v_i^n) - 2\hat{F}_{i+1/2}^n}{v_{i+1}^n - v_i^n}(v_{i+1}^n - v_i^n) \\
&\qquad\qquad - f(v_i^n) - f(v_{i-1}^n) + \frac{f(v_i^n) + f(v_{i-1}^n) - 2\hat{F}_{i-1/2}^n}{v_i^n - v_{i-1}^n}(v_i^n - v_{i-1}^n)\Bigg) \qquad (16a) \\
&\quad = \hat{v}_i^n - v_i^n - \frac{\Delta t^n}{2\Delta x}\Bigg(\left(B_{i+1/2}^n - Q_{i+1/2}^n\right)\Delta v_{i+1/2}^n \\
&\qquad\qquad + \left(B_{i-1/2}^n + Q_{i-1/2}^n\right)\Delta v_{i-1/2}^n\Bigg). \qquad (16b)
\end{aligned}
$$

We point out that the term $\hat{v}_i^n - v_i^n$ is new and accounts for the mesh reconstruction and solution update steps of the MAS (2.1).
We now express $\hat{v}_i^n - v_i^n$ in a conservative form with respect to $\{v_j^n\}$. Accordingly the size of C_i changes as:

$$
h_i^{n+1} = h_i^n + \Delta x_{i+1/2}^{n+1/2} - \Delta x_{i-1/2}^{n+1/2}, \qquad (17)
$$

and the mass of u over C_i as:

$$
\begin{aligned}
h_i^{n+1}\hat{u}_i^n = h_i^n u_i^n &- \left(\Delta x_{i+1/2}^{n+1/2}\right)_- u_i^n + \left(\Delta x_{i+1/2}^{n+1/2}\right)_+ u_{i+1}^n \\
&+ \left(\Delta x_{i-1/2}^{n+1/2}\right)_- u_{i-1}^n - \left(\Delta x_{i-1/2}^{n+1/2}\right)_+ u_i^n. \qquad (18)
\end{aligned}
$$

Now, (18) recasts to:

$$
\begin{aligned}
\hat{v}_i^n = v_i^n &- \frac{\left(\Delta x_{i+1/2}^{n+1/2}\right)_-}{h_i^n} v_i^n + \frac{\left(\Delta x_{i+1/2}^{n+1/2}\right)_+}{h_{i+1}^n} v_{i+1}^n \\
&+ \frac{\left(\Delta x_{i-1/2}^{n+1/2}\right)_-}{h_{i-1}^n} v_{i-1}^n - \frac{\left(\Delta x_{i-1/2}^{n+1/2}\right)_+}{h_i^n} v_i^n.
\end{aligned}
$$

This relation can also be written as a conservative difference

$$
\begin{aligned}
\hat{v}_i^n - v_i^n = &\left(\frac{\left(\Delta x_{i-1/2}^{n+1/2}\right)_-}{h_{i-1}^n} v_{i-1}^n - \frac{\left(\Delta x_{i-1/2}^{n+1/2}\right)_+}{h_i^n} v_i^n \right) \\
&- \left(\frac{\left(\Delta x_{i+1/2}^{n+1/2}\right)_-}{h_i^n} v_i^n - \frac{\left(\Delta x_{i+1/2}^{n+1/2}\right)_+}{h_{i+1}^n} v_{i+1}^n \right) \qquad (19) \\
= &H_{i-1/2}^n - H_{i+1/2}^n \qquad (20)
\end{aligned}
$$

Replacing (20) in (16b) we obtain

$$\begin{aligned} v_i^{n+1} - v_i^n =& H_{i-1/2}^n - H_{i+1/2}^n \\ & - \frac{\Delta t^n}{2\Delta x}\Big(\left(B_{i+1/2}^n - Q_{i+1/2}^n\right) \Delta v_{i+1/2}^n + \left(B_{i-1/2}^n + Q_{i-1/2}^n\right) \Delta v_{i-1/2}^n \Big), \end{aligned} \tag{21}$$

which can be analogously written as a conservative update over the reference uniform mesh

$$v_i^{n+1} = v_i^n - \frac{\Delta t^n}{\Delta x}\left(\frac{\Delta x}{\Delta t^n} H_{i+1/2}^n + \hat{F}_{i+1/2}^n - \frac{\Delta x}{\Delta t^n} H_{i-1/2}^n - \hat{F}_{i-1/2}^n \right). \tag{22}$$

We note that the conservative difference $H_{i-1/2}^n - H_{i+1/2}^n$ accounts for the mesh reconstruction and the solution update step of the MAS.
In order to simplify the presentation of the rest of the proof we assume that the entropy and the conservative variables ($\tilde{v}$ and v, respectively) coincide, i.e. we choose $U(u) = \frac{1}{2}u^2$ for the entropy function. Now, to recover the entropy-entropy flux representation of (21), we multiply it by the entropy variables $\tilde{v}_i^n$, yielding

$$\begin{aligned} U(v_i^{n+1}) - U(v_i^n) + \frac{\Delta t^n}{\Delta x}\left(G_{i+1/2}^n - G_{i-1/2}^n\right) & \\ = M_i^n - \frac{\Delta t^n}{\Delta x}\mathcal{E}_i^{(x)} + \mathcal{E}_i^{(FE)}\left(\Delta v^{n+1/2}\right) & \end{aligned} \tag{23}$$

where G is the numerical entropy flux. We have further following [39],

$$\begin{aligned} \mathcal{E}_i^{(x)} &= \frac{1}{4}\left[D_{i-1/2}\Delta v_{i-1/2}^2 + D_{i+1/2}\Delta v_{i+1/2}^2 \right], \\ \mathcal{E}_i^{(FE)} &\leq \frac{K^3}{4}\left(\frac{\Delta t^n}{\Delta x}\right)^2 \Big[\left(B_{i+1/2} - Q_{i+1/2}\right)^2 \Delta v_{i+1/2}^2 \\ &\qquad + \left(B_{i-1/2} + Q_{i-1/2}\right)^2 \Delta v_{i-1/2}^2 \Big] \\ &\leq \frac{K^3}{4}\left(\frac{\Delta t^n}{\Delta x}\right)^2 \Big[\left(B_{i+1/2} - Q_{i+1/2}^* - D_{i+1/2}\right)^2 \Delta v_{i+1/2}^2 \\ &\qquad + \left(B_{i-1/2} + Q_{i-1/2}^* + D_{i-1/2}\right)^2 \Delta v_{i-1/2}^2 \Big]. \end{aligned}$$

For the derivation of the last inequality we refer to Appendix A. Now, (23) reduces to

$$\begin{aligned} U(v_i^{n+1}) - U(v_i^n) + \frac{\Delta t^n}{\Delta x}\left(G_{i+1/2}^n - G_{i-1/2}^n\right) & \\ \leq M_i^n - \frac{\Delta t^n}{4\Delta x}\left(D_{i-1/2}\Delta v_{i-1/2}^2 + D_{i+1/2}\Delta v_{i+1/2}^2 \right) & \\ + \frac{K^3}{4}\left(\frac{\Delta t^n}{\Delta x}\right)^2 \Big[\left(B_{i+1/2} - Q_{i+1/2}^* - D_{i+1/2}\right)^2 \Delta v_{i+1/2}^2 & \\ + \left(B_{i-1/2} + Q_{i-1/2}^* + D_{i-1/2}\right)^2 \Delta v_{i-1/2}^2 \Big], & \end{aligned}$$

Hence, the sufficienct condition for entropy stability reads

$$M_i^n \leq \frac{\Delta t^n}{4\Delta x}\Bigg\{ \left(D_{i-1/2}^n - K^3 \frac{\Delta t^n}{\Delta x}\left(B_{i-1/2} + Q_{i-1/2}^* + D_{i-1/2} \right)^2 \right) \left(\Delta v_{i-1/2}^n \right)^2 + \left(D_{i+1/2}^n - K^3 \frac{\Delta t^n}{\Delta x}\left(B_{i+1/2} - Q_{i+1/2}^* - D_{i+1/2} \right)^2 \right) \left(\Delta v_{i+1/2}^n \right)^2 \Bigg\}.$$

□

In view of (22) we point out that we can define a conservative numerical scheme to include and describe both the time evolution as well as the adaptation of the mesh. Such a formulation was missing in previous works dealing with the analysis of moving mesh methods. Such a formulation can be given for both the adaptive -as well as for the underlying uniform- mesh-solution pair.

Definition 3.1 (Effective Conservative Scheme)**.** The conservative numerical scheme for the cell averages of the adaptive mesh-solution pair $\left\{M_x^n, U^n\right\}$

$$u_i^{n+1} = \frac{h_i^n}{h_i^{n+1}} u_i^n - \frac{\Delta t^n}{h_i^{n+1}} \left(\mathcal{F}_{i+1/2}^n - \mathcal{F}_{i-1/2}^n \right), \tag{24}$$

where $\mathcal{F}_{i+1/2}^n = \frac{\Delta x}{\Delta t^n} H_{i+1/2}^n + \hat{F}_{i+1/2}^n$. Here $H_{i+1/2}^n$, $\hat{F}_{i+1/2}^n$ are given by (14e) and (13) is defined to be the *Effective Conservative Scheme* of the mesh-solution pair $\{M_x^n, U^n\}$ and the MAS 2.1.

Similarly, the conservative numerical scheme for the reference uniform mesh-solution pair $\left\{\bar{M}, V^n\right\}$

$$v_i^{n+1} = v_i^n - \frac{\Delta t^n}{\Delta x} \left(\mathcal{F}_{i+1/2}^n - \mathcal{F}_{i-1/2}^n \right) \tag{25}$$

is defined as the *Reference Conservative Scheme* of the reference uniform mesh-solution pair as given in Definition 2.2 .

We refer to Figure 2 for a graphical comparison between the non-uniform mesh-solution pair and the corresponding reference uniform mesh-solution pair.

To further explain some of the ingredients of the previous proof we provide and example describing the changes of the grid due to the adaptation of the mesh.

Remark 3.1. To gain further insight into (17), (20) we refer to Figure 3 and provide three special examples of special movement and the corresponding computations of $\hat{v}_i^n - v_i^n$.

- Cell moves to the left.
  This means that $\Delta x_{i+1/2}^{n+1/2} = -r_i^n$, $\Delta x_{i-1/2}^{n+1/2} = -r_{i-1}^n$, so $h_i^{n+1} = h_i^n - r_i^n + r_{i-1}^n = r_{i-1}^n + l_i^n$. The mass of u satisfies $h_i^{n+1}\hat{u}_i^n = r_{i-1}^n u_{i-1}^n + l_i^n u_i^n$; writing in v variables $\hat{v}_i^n = \frac{r_{i-1}^n}{h_{i-1}^n} v_{i-1}^n + \frac{l_i^n}{h_i^n} v_i^n$ or

$$\hat{v}_i^n - v_i^n = \frac{r_{i-1}^n}{h_{i-1}^n} v_{i-1}^n - \frac{r_i^n}{h_i^n} v_i^n. \tag{26}$$

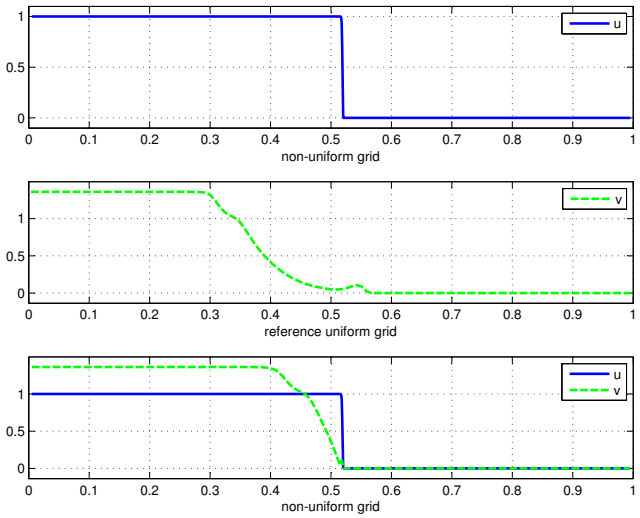

Figure 2: In the first graph the numerical solution of a Burgers problem with discontinuous initial condition over a non-uniform adaptively redefined mesh according to the MAS is depicted. In the second graph we have depicted the corresponding solution over the uniform reference mesh; the relation between the non-uniform and the uniform solution is the per-cell mass conservation. In the third graph, both solutions are presented over the non-uniform grid.

- Cell moves to the right.
  This means that $\Delta x_{i+1/2}^{n+1/2} = l_{i+1}^n$, $\Delta x_{i-1/2}^{n+1/2} = l_i^n$, so $h_i^{n+1} = h_i^n + l_{i+1}^n - l_i^n = r_i^n + l_{i+1}^n$. In this case, the mass of u satisfies $h_i^{n+1}\hat{u}_i^n = r_i^n u_i^n + l_{i+1}^n u_{i+1}^n$, or in v variables $\hat{v}_i^n = \frac{r_i^n}{h_i^n} v_i^n + \frac{l_{i+1}^n}{h_{i+1}^n} v_{i+1}^n$, or

$$\hat{v}_i^n - v_i^n = -\frac{l_i^n}{h_i^n} v_i^n + \frac{l_{i+1}^n}{h_{i+1}^n} v_{i+1}^n. \tag{27}$$

- Cell moves to both directions.
  Similarly, $\Delta x_{i+1/2}^{n+1/2} = l_{i+1}^n$, $\Delta x_{i-1/2}^{n+1/2} = -r_{i-1}^n$, so $h_i^{n+1} = h_i^n + l_{i+1}^n + r_{i-1}^n$. Moreover $h_i^{n+1}\hat{u}_i^n = r_{i-1}^n u_{i-1}^n + h_i^n u_i^n + l_{i+1}^n u_{i+1}^n$, or $\hat{v}_i^n = \frac{r_{i-1}^n}{h_{i-1}^n} v_{i-1}^n + v_i^n + \frac{l_{i+1}^n}{h_{i+1}^n} v_{i+1}^n$, or

$$\hat{v}_i^n - v_i^n = \frac{r_{i-1}^n}{h_{i-1}^n} v_{i-1}^n + \frac{l_{i+1}^n}{h_{i+1}^n} v_{i+1}^n. \tag{28}$$

Let us point that now the conditions (26)-(28) are simple enough in order to be tested for a moving mesh algorithm.

4 Numerical experiments

We perform here a series of numerical experiments to analyze the inequality that appears in Theorem 3.1. To this end we first study the "new" term M_i^n and then the full inequality (15).

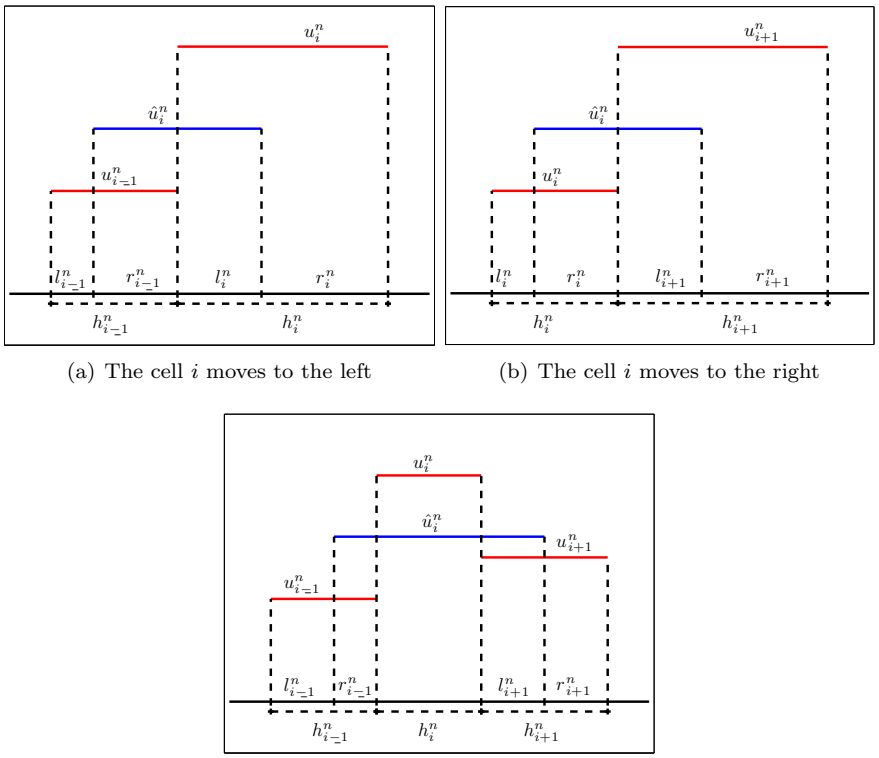

(a) The cell i moves to the left

(b) The cell i moves to the right

(c) The cell i moves to both directions

Figure 3: Three cases of cell movement.

4.1 Experimental study of the M_i^n term

In this section we study the numerical behavior of the M_i^n term given in (14f) under the influence of cell movement and the geometry of the numerical solution. To this end we have constructed a numerical method driving the movement of the cells. The cells move with a prescribed velocity; after each movement the numerical solution is reconstructed in a mass conservative manner over the new grid. Time evolution has been suppressed in order to isolate the effect of the cell movement on M_i^n.

We present the results of the numerical experiment in Figure 4, where in the first case we consider a constant node velocity and an initial solution profile that is comprised of an increasing, a constant, and a decreasing part. Since the velocity of cells movement is kept constant any changes in the sign on M_i^n are due to the geometry of the solution itself. In the second case the node velocity is given by the gradient of the numerical solution. The initial profile used is the same as in the first case.

In both cases we see that M_i^n increases as the cells move towards higher values of the solution profile and decreases as the cells move towards lower values of the solution profile. This verifies the discussion from Remark 3.1.

After investigating the dynamics of the term M_i^n our main goal in the next subsection will be to numerically study the inequality (15).

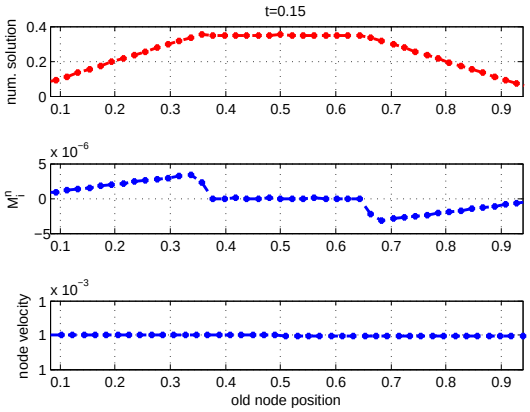

(a) Constant node velocity

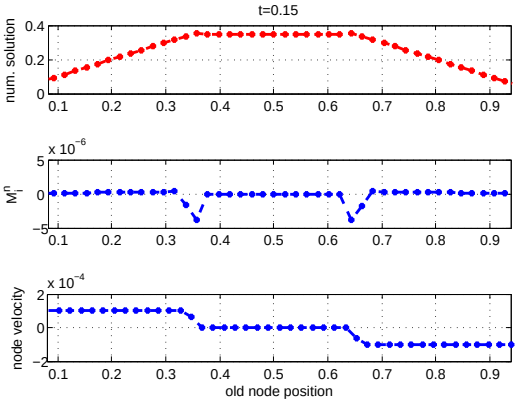

(b) Gradient adjusted node velocity

Figure 4: The effect that the geometry of the solution and the movement of the nodes have on M_i

4.2 Experimental study of inequality (15)

We discretize the domain in cells

$$M_x^n = \{C_i^n, |C_i^n| = h_i^n, i = 1, \dots, N\},$$

where the numerical solution attains the average values

$$U^n = \{u_i^n, i = 1, \dots, N\}.$$

The finite volume scheme we use for the time update (Step 3 of MAS) is written as

$$u_i^{n+1} = \hat{u}_i^n - \frac{\Delta t^n}{h_i^{n+1}} \left(\hat{F}_{i+1/2}^n - \hat{F}_{i-1/2}^n \right),$$

where the numerical flux F is decorated with $\hat{}$ since it is computed over $\hat{U} = \{\hat{u}_i^n, i = 1, \dots, N\}$. $\hat{U}^n$ is the mass conservative reconstruction of U^n over M_x^{n+1}

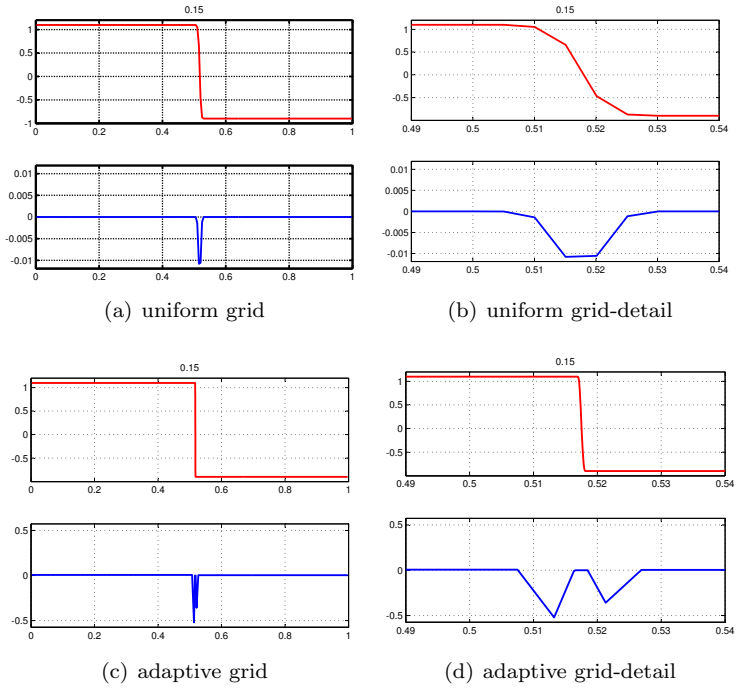

(a) uniform grid (b) uniform grid-detail

(c) adaptive grid (d) adaptive grid-detail

Figure 5: Numerical experiments with the local LxF scheme (29) with parameters CFL=0.8, N=200, K=1, pw=0.097, t=0.15. Sub-figures (a) and (b) correspond to the uniform mesh case and sub-figures (c) and (d) to the adaptive mesh case. In every sub-figure, the first graph is the numerical solution, and the second the corresponding "inequality". In this test case both the uniform and the adaptive versions of the scheme are free of oscillations and the corresponding inequalities carry the proper sign. It is to note however that the discontinuity is resolved in the adaptive mesh case in over a much smaller domain.

according to the MAS:

$$\left\{M_x^n, U^n\right\} \xrightarrow{\text{mesh adapt.}} \left\{M_x^{n+1}, \hat{U}^n\right\} \xrightarrow{\text{num. scheme}} \left\{M_x^{n+1}, U^{n+1}\right\}.$$

The mesh adaptation that we employ follows the steps of MAS; for the mesh adaptation we use the geometric curvature as estimator function. For further information on the implementation, the properties, and for a wide range of numerical experiments using MAS we refer to [4, 6, 3, 5, 36, 35].

In this subsection we will analyse whether (15) holds for various standard numerical schemes for hyperbolic conservation laws when our moving mesh technique is applied. The schemes that we will consider are:

- the local Lax-Friedrichs (lLxF) scheme:

$$\hat{F}_{i+1/2}^n = \frac{f(\hat{u}_i^n) + f(\hat{u}_{i+1}^n)}{2} - 0.5 \ \max\left(|\hat{u}_i^n|, |\hat{u}_{i+1}^n|\right) \ \left(\hat{u}_i^n - \hat{u}_{i+1}^n\right), \quad (29)$$

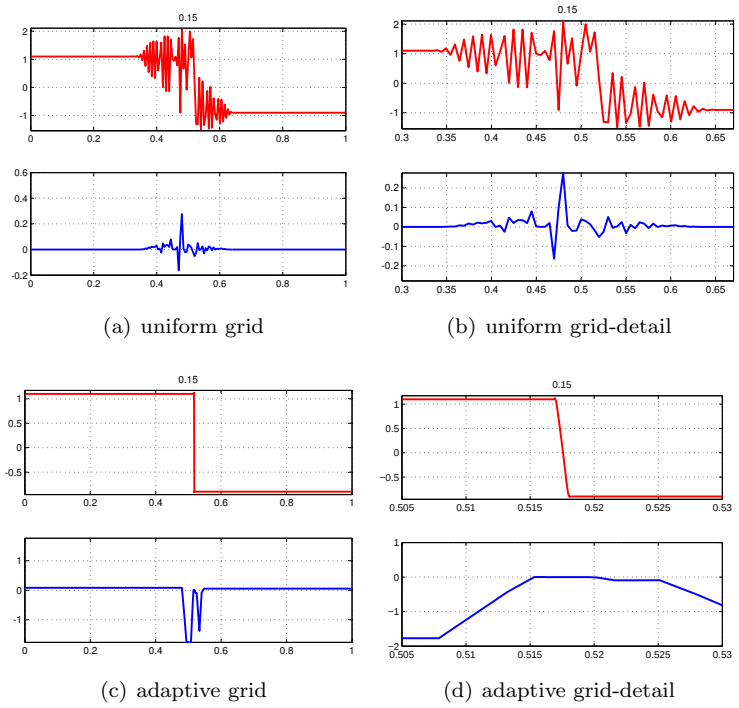

(a) uniform grid (b) uniform grid-detail

(c) adaptive grid (d) adaptive grid-detail

Figure 6: Numerical experiments with the FTCS scheme (30) with parameters CFL=0.5, N=200, K=1, pw=0.097, t=0.15. In parallel depictions of the numerical solution (first graph in every sub-figure) along side with the inequality (second graph in every sub-figure). The uniform mesh case exhibits spurious oscillations due to the anti-diffusive nature of the FTCS scheme; the corresponding inequality oscillates in the sign as well. On the other hand, the adaptive mesh case is free of oscillations and the sign of the inequality is the correct one along the shock.

- the Forward in Time Central in Space (FTCS) scheme:

$$\hat{F}^n_{i+1/2} = \frac{f(\hat{u}^n_i) + f(\hat{u}^n_{i+1})}{2}, \tag{30}$$

- the Lax-Wendroff (LxW) scheme:

$$\hat{F}^n_{i+1/2} = f\left(\frac{h^n_{i+1}\,\hat{u}^n_{i+1} + h^n_i\,\hat{u}^n_i}{h^n_{i+1} + h^n_i} - \frac{\Delta t^n}{h^n_{i+1} + h^n_i}\left(f(\hat{u}^n_{i+1}) - f(\hat{u}^n_i)\right)\right). \tag{31}$$

The results obtained by the adaptive lLxF, FTCS and LxW schemes can bee seen in Figures 5, 6, 7 respectively. Let us rewrite inequality (15) in the following

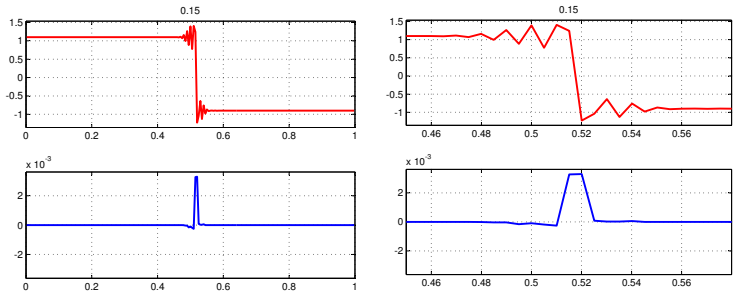

(a) uniform grid (b) uniform grid-detail

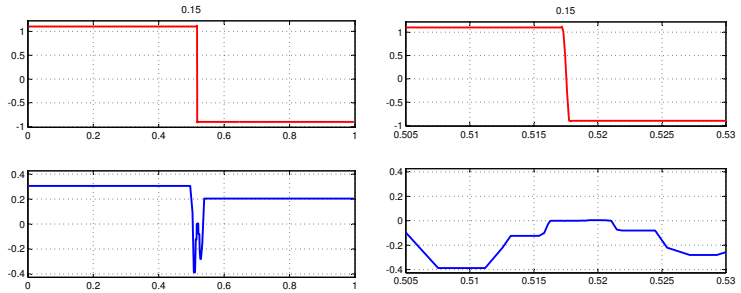

(c) adaptive grid (d) adaptive grid-detai

Figure 7: Numerical experiments with the LxW scheme (31) with parameters CFL=0.8, N=200, K=1, pw=0.097, t=0.15. The oscillations that appear in the uniform mesh case are in this case due to the dispersive nature of the LxW scheme; the sign of the inequality is the wrong one. At the same time the adaptive mesh case is clean of oscillations and the sign of the inequality is correct along the discontinuity of the solution.

way:

$$M_i^n - \frac{\Delta t^n}{4\Delta x}\Bigg\{\left(D_{i-1/2}^n - K^3\frac{\Delta t^n}{\Delta x}\left(B_{i-1/2}+Q_{i-1/2}^*+D_{i-1/2}\right)^2\right)\left(\Delta v_{i-1/2}^n\right)^2 + \left(D_{i+1/2}^n - K^3\frac{\Delta t^n}{\Delta x}\left(B_{i+1/2}-Q_{i+1/2}^*-D_{i+1/2}\right)^2\right)\left(\Delta v_{i+1/2}^n\right)^2\Bigg\} \leq 0. \tag{32}$$

In every (sub-)figure we present the numerical solution obtained over uniform and over adaptive grids; along side we present the graph of the left-hand side of (32).

In the numerical tests, we examine the sign of the LHS of (32) (negative being the correct one) and study the way our mesh adaptation technique is affecting it. In more details, we can see that in the oscillatory scheme cases (FTCS and LxW) the mesh adaptation technique that we use has completely tamed the oscillations of the solution; see [4, 6, 3, 5, 36, 35] for a thorough numerical (as well as analytical) study of the stabilization properties of the MAS that we employ in this work. We moreover see that the sign of the inequality in the

adaptive case is the correct one along the discontinuties. The solutions over uniform mesh are oscillatory due to the anti-diffusive (respectively dispersive) nature of the schemes; the inequality has either oscillatory sign (uniform FTCS) or the wrong sign (uniform LxW).

5 Conclusions

We study in this paper the entropy dissipation property of the adaptive mesh reconstruction techniques. We consider a projection from the physical domain over an underlying uniform mesh. This gives us the opportunity to combine in a single conservative formulation (Effective Conservative Scheme, Definition 3.1) the effect of both time evolution and mesh adaptation. The entropy dissipation of the mesh adaptation appears in Theorem 3.1 in the form of inequality (15) the sign of which we analyse numerically. We verify numerically, by using oscillatory schemes that violate (15) when the mesh is uniform, that the mesh adaptation based on the discrete curvature of the numerical solution and the moving mesh techniques as described in Section 2, cf [35, 3], can give the proper sign in (15) and at the same time tame the oscillatory nature of the scheme.

For future work, our aim is to generalize the above ideas on adaptation of moving for multidimensional problems. On top of the entropy criteria that we have studied in the present work we want to analyze further desirable properties of the numerical solution, the numerical scheme, and most notably of the underlying mesh that should be preserved.

Aknowledgements
The authors wish to thank E. Tadmor and Ch. Makridakis for the very useful discussions and suggestions. This work has been partially supported by the research center of Computational Sciences in Mainz as well as by the Humboldt foundation. The authors gratefully acknowledge their support.

Appendices

A Entropy stable schemes

In this section we present parts -after some modifications- of the analysis conducted in [38, 39]. We moreover note that these works are to be viewed in the context of the seminal works on the subject by [13, 31].

A finite volume approximation of the one-dimensional conservation law is written in the form

$$u_i^{n+1} = u_i^n - \frac{\Delta t^n}{\Delta x}\left(F_{i+1/2}(U^n) - F_{i-1/2}(U^n)\right).$$

The corresponding viscosity form reads

$$u_i^{n+1} - u_i^n = \frac{\Delta t^n}{2\Delta x}\Big\{ -\Big(f(u_{i+1}^n) - f(u_u^n)\Big) + Q_{i+1/2}^n \Delta u_{i+1/2}^n \\ -\Big(f(u_i^n) - f(u_{i-1}^n)\Big) - Q_{i-1/2}^n \Delta u_{i-1/2}^n \Big\} \qquad (33)$$

with the numerical viscosity given by $Q^n_{i+1/2} = \frac{f(u^n_i)+f(u^n_{i+1})-2F^n_{i+1/2}}{\Delta u^n_{i+1/2}}$. After denoting $B_{i+1/2} = \frac{f(u^n_{i+1})-f(u^n_i)}{\Delta u^n_{i+1/2}}$ equation (33) can be rewritten as

$$u^{n+1}_i - u^n_i = -\frac{\Delta t^n}{2\Delta x}\Big(\Big(B_{i+1/2} - Q_{i+1/2}\Big)\Delta u^n_{i+1/2} + \Big(B_{i-1/2} + Q_{i-1/2}\Big)\Delta u^n_{i-1/2}\Big).$$

Now, setting $D_{i+1/2} = Q_{i+1/2} - Q^*_{i+1/2}$, with Q^* the numerical viscosity of an entropy conservative scheme we obtain

$$u^{n+1}_i - u^n_i = -\frac{\Delta t^n}{2\Delta x}\Big(\Big(B_{i+1/2} - Q^*_{i+1/2} - D_{i+1/2}\Big)\Delta v^n_{i+1/2} + \Big(B_{i-1/2} + Q^*_{i-1/2} + D_{i-1/2}\Big)\Delta u^n_{i-1/2}\Big).$$

Next we multiply the last equation with the entropy variables $\tilde{v}$. After noting that

$$\begin{aligned}\left\langle \tilde{v}^n_i, u^{n+1}_i - u^n_i \right\rangle &= U(u^{n+1}_i) - U(u^n_i) - \mathcal{E}^{(FE)}_i(\tilde{v}^{n+1/2}_i),\\ \left\langle \tilde{v}^n_i, F^n_{i+1/2} - F^n_{i-1/2} \right\rangle &= G^n_{i+1/2} - G^n_{i-1/2} + \mathcal{E}^x_i(\tilde{v}^n_i),\end{aligned}$$

where $\mathcal{E}^{(FE)}_i(\tilde{v}^{n+1/2}_i)$, $\mathcal{E}^x_i(\tilde{v}^n_i)$ are given by

$$\begin{aligned}\mathcal{E}^{(FE)}_i(\tilde{v}^{n+1/2}_i) &= \int_{\xi=-1/2}^{\xi=1/2}\left(\frac{1}{2}+\xi\right)\left\langle \Delta\tilde{v}^{n+1/2}_i, H(\tilde{v}^{n+1/2}_i)\Delta\tilde{v}^{n+1/2}_i\right\rangle,\\ \mathcal{E}^x_i(\tilde{v}^n_i) &= \frac{1}{4}\left\langle \Delta\tilde{v}^n_{i-1/2}, D^n_{i-1/2}\Delta\tilde{v}^n_{i-1/2}\right\rangle + \frac{1}{4}\left\langle \Delta\tilde{v}^n_{i+1/2}, D_{i+1/2}\Delta\tilde{v}^n_{i+1/2}\right\rangle,\end{aligned}$$

we arrive to the entropy-entropy flux pair representation

$$U(v^{n+1}_i) - U(v^n_i) + \frac{\Delta t^n}{\Delta x}\left\{F^n_{i+1/2} - F^n_{i-1/2}\right\} = \mathcal{E}^{(FE)}_i(\tilde{v}^{n+1/2}) - \frac{\Delta t^n}{\Delta x}\mathcal{E}^x_i(\tilde{v}^n).$$

Now, entropy stability implies that:

$$\mathcal{E}^{(FE)}_i(\tilde{v}^{n+1/2}) - \frac{\Delta t^n}{\Delta x}\mathcal{E}^x_i(\tilde{v}^n) \le 0. \tag{34}$$

In order to satisfy (34) the following conditions are sought as sufficient

$$\begin{aligned}K^3\frac{\Delta t^n}{\Delta x}(B_{i+1/2} - Q^*_{i+1/2} - D_{i+1/2})^2 &\le D_{i+1/2},\\ K^3\frac{\Delta t^n}{\Delta x}(B_{i-1/2} + Q^*_{i-1/2} + D_{i-1/2})^2 &\le D_{i-1/2}\end{aligned}$$

for every i. Due to conservative symmetry they give

$$K^3\frac{\Delta t^n}{\Delta x}(B_{i+1/2} \pm Q^*_{i+1/2} \pm D_{i+1/2})^2 \le D_{i+1/2} \tag{35}$$

The last relation yields the following results for $c = \frac{\Delta x}{K^3 \Delta t^n}$:

$$D_{i+1/2} \geq 0$$
$$(B \pm Q^* \pm D_{i+1/2})^2 \leq c D_{i+1/2}.$$

This leads to $D_{i+1/2}^2 + (2(Q^* \pm B) - c)D_{i+1/2} + (Q^* \pm B)^2 \leq 0$. By setting $k_1 = Q^* + B$ and $k_2 = Q^* - B$ we get two different quadratic inequalities that need to be satisfied for $D_{i+1/2}$:

$$D_{i+1/2}^2 + (2k_1 - c)D_{i+1/2} + k_1^2 \leq 0 \text{ and } D_{i+1/2}^2 + (2k_2 - c)D_{i+1/2} + k_2^2 \leq 0.$$

The necessary restrictions for the existence of a solution are $c \geq 4k_1$ and $c \geq 4k_2$. This mean that $Q^* \pm B \leq c/4$, i.e $c \geq 4Q^*$ or

$$\frac{\Delta t^n}{\Delta x} \leq \frac{1}{4K^3 Q^*}.$$

References

[1] Ch. Arvanitis. *Finite Elements for Hyperbolic Conservation Laws: New methods and computational techniques.* PhD thesis, University of Crete, 2002.

[2] Ch. Arvanitis. Mesh redistribution strategies and finite element method schemes for hyperbolic conservation laws. *J. Sci. Computing*, 34:1–25, 2008.

[3] Ch. Arvanitis and A. Delis. Behavior of finite volume schemes for hyperbolic conservation laws on adaptive redistributed spatial grids. *SIAM J. Sci. Comput.*, 28:1927–1956, 2006.

[4] Ch. Arvanitis, Th. Katsaounis, and Ch. Makridakis. Adaptive finite element relaxation schemes for hyperbolic conservation laws. *Math. Model. Anal. Numer.*, 35:17–33, 2001.

[5] Ch. Arvanitis, Ch. Makridakis, and N. Sfakianakis. Entropy conservative schemes and adaptive mesh selection for hyperbolic conservation laws. *JHDE*, pages 1–22, 2006.

[6] Ch. Arvanitis, Ch. Makridakis, and A. Tzavaras. Stability and convergence of a class of finite element schemes for hyperbolic systems of conservation laws. *SIAM J. Numer. Anal.*, 42:1357–1393, 2004.

[7] W. Cao, W. Huang, and R. D. Russell. A moving mesh method based on the geometric cosnervation law. *SIAM J. Sci. Comput.*, 24:118–142, 2002.

[8] R. Courant and K. Friedrichs. *Supersonic Flow and Shock Waves.* Springer, 1948.

[9] R. Courant, K. Friedrichs, and H. Lewy. On the partial difference equations of mathematical physics. *IBM Journal*, pages 215–234, 1967. English translation of the 1928 German original.

[10] E. Dorfi and L. Drury. Simple adaptive grids for 1d initial value problems. *J. Computational Physics*, 69:175–195, 1987.

[11] B. Fornberg. Generation of finite difference formulas on arbitrary spaced grids. *Mathematics of Computations*, 51:699–706, 1988.

[12] H. Freistuehler, Chr. Schmeiser, and N. Sfakianakis. Stable length distributions in co-localized polymerizing and depolymerizing protein filaments. *SIAM J. of Applied Math.*, 2011.

[13] K. O. Friedrichs and P. D. Lax. Systems of conservation laws with convex extension. *Proc. Nat. Acad. Sci. USA*, 68:1686–1688, 1971.

[14] M.B. Giles and E. Süli. Adjoint methods for pdes: a posteriori error analysis and post processing by duality. *Acta. Numr.*, 11:145–236, 2002.

[15] E. Godlewski and P. A. Raviart. *Hyperbolic Systems of Conservation Laws*. Ellipses, 1990.

[16] A. Harten and J. Hyman. Self adjusting grid methods for one-dimensional hyperbolic conservation laws. *J. Comput. Physics*, 50:235–269, 1983.

[17] R. Hartmann and P. Houston. Adaptive discontinuous galerkin finite element methods for the compressible euler equations. *J. Comput. Phys.*, 183(2):508–532, 2002.

[18] B. T. Hayes and Ph. LeFloch. Non-classical shocks and kinetic relations: Scalar conservation laws. *Arch. J. Math. Anal.*, 139:1–56, 1997.

[19] G. W. Hedstrom. Models of difference schemes for $u_t + u_x = 0$ by partial differential equations. *J. Comput. Physics*, 50:235–269, 1983.

[20] C. W. Hirt. Heuristic stability theory for finite difference schemes. *J. Comput. Physics*, 2:339–355, 1968.

[21] D. Kroener. *Numerical schemes for Conservation Laws*. Wiley Teubner, 1997.

[22] D. Kröner and M. Ohlberger. A posteriori error estimates for upwind finite volume schemes for nonlinear conservation laws in multidimensions. *Math. Comput.*, 69(229):25–39, 2000.

[23] A. Kurganov, G. Petrova, and B. Popov. Adaptive semidiscrete central-upwind schemes for nonconvex hyperbolic conservation laws. *SIAM J. Sci. Comput.*, 29(6):2381–2401 (electronic), 2007.

[24] P. D. Lax. Weak solutions of nonlinear hyperbolic equations and their numerical computation. *Comm. pure and applied mathematics*, 7:159–193, 1954.

[25] P. D. Lax and R. Richtmyer. Survey of the stability of linear finite difference equations. *Comm. Pure Appl. Math.*, 9:267–293, 1956.

[26] P. D. Lax and B. Wendroff. Systems of conservation laws. *Comm. Pure Appl. Math.*, 13:217–237, 1960.

[27] Ph. LeFloch and Ch. Rohde. High-order schemes, entropy inequalities and nonclassical shocks. *J. Numerical Analysis SIAM*, pages 2023–2060, 2000.

[28] R. LeVeque. *Numerical methods for Conservation Laws*. Birkhauser Verlag, second edition, 1992.

[29] R. LeVeque. *Finite volume methods for hyperbolic problems*. Cambridge texts in applied mathematics, first edition, 2002.

[30] M. Lukáčová-Medviďová and E. Tadmor. On the entropy stability of the roe-type finite volume methods. *Proc. Symp. Appl. Math.*, 67:765–774, 2009.

[31] M.S. Mock. Some higher order difference schemes enforcing an entropy inequality. *Michigan Math.J.*, 25:325–344, 1978.

[32] M. Ohlberger. A review of a posteriori error control and adaptivity for approximations of non-linear conservation laws. *Int. J. Numer. Methods Fluids*, 59(3):333–354, 2009.

[33] O. Oleinik. Discontinuous solutions of non-linear differential equations. *AMS Transactions Series 2*, pages 95–172, 1963.

[34] G. Puppo and M. Semplice. Entropy and the numerical integration of conservation laws. *Commun. Comput. Phys.*, pages 1–28, 2011.

[35] N. Sfakianakis. *Finite Difference schemes on Non-Uniform Meshes for hyperbolic Conservation Laws*. PhD thesis, University of Crete, 2009.

[36] N. Sfakianakis. Adaptive mesh reconstruction for hyperbolic conservation laws with total variation bound. *Math. Comput.*, 2011.

[37] J. Smoller. *Shock Waves and Reaction-Diffusion Equations*. Springer-Verlag, 1991.

[38] E. Tadmor. The numerical viscosity of entropy stable schemes for systems of conservation laws. *Math. Comput.*, pages 91–103, 1987.

[39] E. Tadmor. Entropy stability theory for difference approximations of non-linear conservation laws and related time dependent problems. *Acta Numerica*, pages 451–512, 2003.

[40] H. Tang and T. Tang. Adaptive mesh methods for one- and two-dimensional hyperbolic conservation laws. *SIAM J. Numerical Analysis*, 41:487–515, 2003.

[41] H.Z. Tang and G. Warnecke. High resolution schemes for conservation laws and convection diffusion equations with varying time and space grids. *J. Comput. Math.*, 24(2):121–140, 2006.

[42] J.W Thomas. *Numerical partial differential equations - Finite difference methods*. Springer, 1995.

[43] J.W Thomas. *Numerical partial differential equations - Conservation laws and elliptic equations*. Springer, 1999.

[44] P. D. Thomas and C. K. Lombard. Numerical solution of the one-dimensional hydrodynamic equations in an arbitrarytime-dep endent coordinate system. *AIAA J.*, 17:10301037, 1979.

[45] E.F. Toro. *Shock-capturing methods for free-surface shallow flows*. Wiley, 2001.

[46] J. G. Trullio and K. R. Trigger. Numerical solution of the one-dimensional hydrodynamic equations in an arbitrarytime-dep endent coordinate system. *Report UCLR-6522, Lawrence Radiation Laboratory, University of California, Berkeley*, 1961.

[47] R. F. Warming and B. J. Hyett. The modified equation approach to the stability and accuracy of finite difference methods. *J. Comp. Physics*, 14:159–179, 1974.